# Shape optimization of a control arm for additive manufacturing with fiber reinforcement

Paula Andrea Chacón Santamaría

Trabajo de grado para optar al título de Ingeniera Mecánica

Director
Octavio Andrés González Estrada
Ingeniero mecánico, PhD.

Codirector
Alejandro Sierra Vargas
Ingeniero mecánico

Universidad Industrial de Santander
Facultad de Ingenierías físico-mecánicas
Escuela de Ingeniería mecánica
Bucaramanga
2019

**Acknowledgements**

First, I want to thank my parents, Laura and Gilberto, for giving me this opportunity to become a professional, for educated me, for making me the person I am. Without them, none of this would have been possible. I also want to thank the rest of my family for giving me support, strength and always believing in me.

I am also grateful to my director Andrés González and my co-director Alejandro Sierra for giving me their knowledge, wisdom and time for the development of this work. Finally, I want to thank the Industrial University of Santander for giving me a quality education, for helping me to develop as much as a professional as a person.

**Contents**

Page

## List of Tables

Page

## List of Figures

Page

## List of Appendices

(The appendices are attached to the CD and can be viewed in the database of UIS library)

Appendix A. Stress analysis of a suspension control arm.

Appendix B. Topology optimization of a suspension control arm.

## RESUMEN

**TÍTULO:** OPTIMIZACIÓN DE FORMA DE UN BRAZO DE SUSPENSIÓN PARA MANUFACTURA ADITIVA CON REFUERZO DE FIBRA.[*]

**AUTOR:** PAULA ANDREA CHACÓN SANTAMARÍA.[**]

**PALABRAS CLAVE:** MANUFACTURA ADITIVA, REFUERZO DE FIBRA, MÉTODO DE ELEMENTOS FINITOS, OPTIMIZACIÓN DE FORMA, BRAZO DE SUSPENSIÓN, TENSIÓN DE VON MISES.

**DESCRIPCIÓN:** El sistema de suspensión de un vehículo absorbe energía para mejorar las condiciones de conducción en terrenos irregulares, también apoya su carrocería y la protege contra daños. Algunos de los componentes que permiten el correcto funcionamiento del sistema son los brazos o tijeras de la suspensión. Este estudio tiene como objetivo determinar la distribución de tensiones de un brazo de la suspensión trasera de un vehículo tipo buggy, para realizar una optimización topológica de la pieza para ser producida por manufactura aditiva con refuerzo de fibra. Los procedimientos de optimización se complementan con la manufactura aditiva para crear piezas funcionales, reduciendo la cantidad de material utilizado. La geometría de la suspensión se modeló para encontrar las cargas aplicadas en el brazo a través de un análisis cinético. Como resultado, las cargas se obtuvieron en función del tiempo. De estos valores, se seleccionaron dos tiempos críticos para realizar los análisis. Las tensiones máximas de von Mises se evaluaron como 22 MPa y 20 MPa para cada tiempo, que son valores bajos considerando la resistencia del acero, el material actual de la pieza. Luego, se llevó a cabo la optimización del brazo de suspensión. Los nuevos materiales seleccionados fueron nylon con refuerzo de fibra de vidrio. La tensión máxima de von Mises para el modelo optimizado fue de 2.7 MPa. Finalmente, la pieza optimizada fue fabricada mediante manufactura aditiva y probada con éxito en el carro tipo buggy. El peso del prototipo final fue de 216 g, que es casi un 75% menos que la parte de acero.

[*] Trabajo de grado.

[**] Facultad de Ingenierías Físico-Mecánicas. Escuela de Ingeniería Mecánica. Director: Octavio Andrés González Estrada, PhD. Codirector: Alejandro Sierra Vargas, Ingeniero mecánico.

## ABSTRACT

**TITLE:** SHAPE OPTIMIZATION OF A CONTROL ARM FOR ADDITIVE MANUFACTURING.*

**AUTHOR:** PAULA ANDREA CHACÓN SANTAMARÍA.**

**KEYWORDS:** ADDITIVE MANUFACTURING, FIBER REINFORCEMENT, FINITE ELEMENT METHOD, SHAPE OPTIMIZATION, CONTROL ARM, VON MISES STRESS.

**DESCRIPTION:** The suspension system of a vehicle absorbs energy to improve driving conditions in irregular terrains, also supports its bodywork and protect it from damage. Some of the components that allow the correct performance of the system are the control arms. This study aims to determine the stress distribution of a control arm of the rear suspension of a buggy vehicle, to perform a topology optimization of the part to be produce by Additive Manufacturing (AM) with fiber reinforcement. Optimization procedures are complemented with AM to create functional parts, reducing the amount of material used. The suspension geometry was modeled in order to find the loads applied on the control arm through a kinetic analysis. As a result, the loads were obtained as a function of time. From these values, two critical times were selected to perform the analyzes. The maximum von Mises stresses were evaluated as 22 MPa and 20 MPa for each time, which are low values considering the strength of steel, the current material of the part. Then, the optimization of the control arm was carried out. The new materials selected were nylon with fiberglass reinforcement. The von Mises maximum stress for the optimized model was 2.7 MPa. Finally, the optimized part was manufactured by AM and successfully tested in the buggy car. The weight of the final prototype was 216 g, which is nearly 75% less than the steel part.

---

* Bachelor Thesis.

** Facultad de Ingenierías Físico-Mecánicas. Escuela de Ingeniería Mecánica. Director: Octavio Andrés González Estrada, PhD. Codirector: Alejandro Sierra Vargas, Ingeniero mecánico.

## Introduction

Manufacturing is the basis of the national economy in many countries and, throughout history, industry has favored national wealth development. Many component designs of different products that are currently commercialized are limited by traditional manufacturing processes. In industry, casting, plastic deformation and material removal operations are commonly used, these are the most traditional ones. But, they do not allow design flexibility since they cannot achieve complex shapes. Some complications presented in subtractive manufacturing are the need for fixtures, diverse tooling, the possibility of collisions and difficulty of the cutter in reaching deeper and invisible zones (Karunakaran, Bernard, Suryakumar, Dembinski, & Taillandier, 2012). Other traditional processes, *e.g.*, pressing, casting, forming, impose additional design constraints to those inherited by the subtractive techniques used to fabricate the required tools and patterns (Gao *et al*., 2015). This means that custom designs could be expensive and difficult to manufacture.

Additionally, it is necessary to use alternative manufacturing processes and materials to reduce the environmental impact (Vinodh & Jayakrishna, 2011), since many conventional procedures tend to release toxic or contaminating substances, which without proper processing can destroy entire ecosystems and inflict severe damage on the health of consumers and workers. They also generate large amounts of waste material, especially material removal processes, when manufacturing parts with shape complexity (Paris, Mokhtarian, Coatanéa, Museau, & Ituarte, 2016).

The development of Additive Manufacturing (AM) makes possible to overcome limitations and supposes a transformation with respect to the traditional processes, allowing to manufacture by controlled deposition of material, adding exclusively where it is necessary. The first AM machine

was developed in 1986 by Charles Hull, using a process known as stereolithography (Ngo, Kashani, Imbalzano, Nguyen, & Hui, 2018). Nowadays, there are different AM methods, which could be divided into the following groups: vat photopolymerization, powder bed fusion, material extrusion, material jetting, binder jetting, sheet lamination, and directed energy deposition (Gao *et al*., 2015). Additive manufacturing is changing the way products are designed and manufactured. It provides the necessary design freedom, favoring the creation of innovative products and making possible the manufacture of new shapes and complex geometries with customizable material properties, such as those resulting from shape or topology optimization (Khode, Senthilkumar, Patil, Kulkarni, & Trikande, 2017).

Another shift in design paradigm is the use of shape optimization processes to obtain the lowest possible weight, often performing a Finite Element Analysis (FEA). The Finite Element Method (FEM) together with optimization procedures generates superior part designs. Thus, optimization is an appropriate approach when designing for AM, this has been previously exemplified in (Chen *et al*., 2015) (Walton & Moztarzadeh, 2017). While carrying out this design process for AM through shape optimization, certain principles, methodologies, and recommendations must be taken into account (Vayre, Vignat, & Villeneuve, 2012) (Allaire, Dapogny, Faure, & Michailidis, 2017). Likewise, it is necessary to look for the minimum use of support material but ensuring manufacturability (Leary, Merli, Torti, Mazur, & Brandt, 2014). Additive manufacturing opens the possibility of rethinking the designs of some products, in order to decrease their weight and thus save material. This manufacturing process is attractive to weight sensitive applications at industries such as aerospace, automotive, sports, among others. Dama, Malyala, Babu, Rao, & Shaik (2017) presented an example in which a structure of an automotive chassis is developed using additive manufacturing.

In the process of redesigning structural or machinery components, it is essential to consider the importance of material strength, so that the parts can fulfill their function. Composite materials allow to combine the properties of various materials by synthesizing a new material with better properties. Composites extend the reach of AM by considering the use of fiber reinforcement (Hegab, 2016) (Spowart, Gupta, & Lehmhus, 2018). Fiber reinforced composite structures have been employed in various engineering applications because of their very high strength-to-weight ratio. Fiber reinforcement perfectly complements the design for additive manufacturing, to produce highly customized parts with significantly improved mechanical properties. But, there are some problems that must be addressed including void formation, poor adhesion of fibers and matrix, blockage due to filler inclusion, increased curing time, modeling, simulation, among others (Parandoush & Lin, 2017). Besides, it is also important to take into consideration the proper fiber placement, fiber seizing, and the correct selection of materials, aspects that significantly influence at the time of manufacturing and testing (Hofstätter, Pedersen, Tosello, & Hansen, 2017).

One of the methods that can be benefited by fiber reinforcement is Fused Deposition Modeling (FDM), which is one of the most used in AM. Since this method only uses thermoplastic materials, its resulting parts have limited mechanical properties. But, fiber reinforcement can improve these properties, principally tensile strength and Young's modulus (Ning, Cong, Qiu, Wei, & Wang, 2015).

The use of composite materials with continuous fiber reinforcement can produce more satisfactory results than the utilization of short fiber (Blok, Longana, Yu, & Woods, 2018), generating parts with a higher-grade design and improved functionality. A technology developed by Markforged (Mark & Gozdz, 2015) allows using continuous fiber reinforcement in AM. The elastic properties of 3D printed structures made with this technology have been evaluated, and

models to predict them have been developed (Melenka, Cheung, Schofield, Dawson, & Carey, 2016). Additionally, failure modes and damage (Al Abadi, Thai, Paton-Cole, & Patel, 2018), as well as other properties like interlaminar shear strength (Caminero, Chacón, García Moreno, & Reverte, 2018), and effects of part orientation, number of fiber layers, and fiber layer proximity (Sauer, 2018) have been researched.

In the automotive industry, the application of continuous fiber reinforcement, in combination with shape optimization for additive manufacturing, can produce parts with higher performance. A control arm of a car suspension was selected to carry out this study. For this part, optimization, simulation, and analysis processes have already been performed in (B. C. Song, Park, Kang, & Lee, 2009) (X. G. Song et al., 2010) (Bouazara, 2009). These studies have achieved significant weight reductions without the use of fiber, which can further potentiate these optimization procedures.

On the other hand, as Lederman, Messina, Pienknagura, & Rigolini (2014) mentioned, in Latin America the development of innovative products is urgent for the economic growth of the region. There are many potential reasons why Latin America and the Caribbean (LAC) firms grow as slowly as they do, one is the lack of innovation, LAC firms introduce new products less frequently than firms in otherwise similar economies. Therefore, it is important to promote research in new technologies, such as additive manufacturing, since they are not widely used for applications in the Colombian industry and entrepreneurship. But, they can provide value and differentiation to local products to make them more competitive.

This research aims to perform the shape optimization of a suspension control arm using FEA, in order to be produced by additive manufacturing with fiber reinforcement. For this purpose, initially, the current material, loading conditions and constraints to which the control arm is

subjected were determined, taking into account its traditional design. Secondly, the numerical model and analysis of the part were developed considering its current material and shape to obtain the total displacement and von Mises stress distributions and their maximum values. Then, the new material model was defined and the shape optimization was performed with the goal of maximizing stiffness. Next, the results from the optimization process were validated by manufacturing and testing the part. Finally, conclusions were formulated.

# 1. Objectives

## 1.1. General Objective

Perform the shape optimization of a control arm of a car suspension using the finite element method, in order to be produced by additive manufacturing with fiber reinforcement.

## 1.2. Specific Objectives

- Determine the material, load conditions and constraints to which the part is subjected.
- Develop the numerical model and analysis of the part considering its current material and shape to obtain the distributions of von Mises stress and total displacement, and their respective maximum values.
- Define the new material model and perform the shape optimization to maximize the stiffness of the part.
- Validate the results obtained by manufacturing and testing the part.

# 2. Materials and methods

## 2.1. Current control arm model

The suspension system of a buggy car (Figure 1a) was taken as a reference for the study. This system was analyzed to obtain the forces on the lower control arm for the calculation of stresses and displacements with its current design. The geometry of the current model can be seen in Figure 1b. The control arm is made of steel, and its properties are shown in Table 1. This material is one of the most used to construct this mechanical part in commercial automobiles.

Table 1. Structural steel mechanical properties.

| **Property** | **Value** |
|---|---|
| Tensile Ultimate Strength | 460 MPa |
| Tensile Yield Strength | 250 MPa |
| Young's Modulus | 200 GPa |
| Poisson's Ratio | 0.3 |
| Bulk Modulus | $1.67 \times 10^{11}$ Pa |
| Shear Modulus | $7.69 \times 10^{10}$ Pa |

Source. Ansys database (ANSYS Inc., 2018).

The Finite Element Method requires the appropriate definition of boundary conditions and the generation of the mesh for the optimal convergence of the solution. The boundary conditions corresponded to the loads applied to the control arm and its supports. To obtain the reactions in the component that was analyzed, a kinetic analysis was performed using SolidWorks Motion

complement (Dassault Systemes, 2017). In this process, the following parts of the system were modeled:

- Upper control arm.
- Lower control arm.
- Spring shock absorber.
- Ball joints.

The steering knuckle, that is the part between the ball joints, was assumed as a rectangular plate. A quarter-vehicle model was taken into account to perform the study since it is a simple model but widely used in suspension design (Bouazara, 2009). The assembly shown in Figure 1b was used to calculate the reactions in the lower control arm. It should be mentioned that, in the case of this suspension, the spring shock absorber is not connected to the lower arm as usual, but to the upper one. An upward vertical force of 1125 N was applied in the middle of the steering knuckle, this magnitude corresponds to a quarter of the weight of the vehicle (including passengers). For the simulation, the spring stiffness used was 30 N/mm and the damping coefficient of the shock absorber was 0.22 Ns/mm. The calculated forces were the reactions due to the contact with the ball joint.

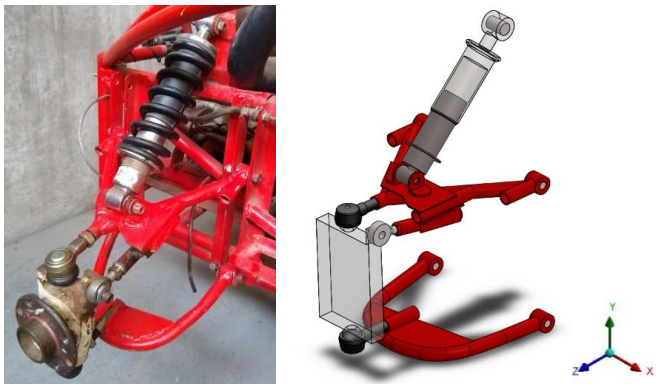

(a) (b)

Figure 1. Real (a) and modeled (b) suspension systems.

Through the kinetic analysis, the variation of the components of the force with respect to time was found. Since the force was not constant, the stress and total displacement distributions were calculated for two different moments, thus, two analyses were carried out. The first one for the initial time and the second one for the steady state. The forces used for both analyses are shown in Table 2.

Table 2. Forces applied for each analysis.

| **Component** | **First analysis** | **Second analysis** |
|---|---|---|
| *x*-component (N) | -2.3 | -2.9 |
| *y*-component (N) | 61 | -10 |
| *z*-component (N) | 32 | -82 |
| Resultant (N) | 68.92 | 82.66 |

The supports taken into account for both analyzes were cylindrical supports. These supports avoid rigid body motion in the static structural analysis. Figure 2 shows the positions were the supports and the force were applied for the first analysis. These positions were the same for the second analysis.

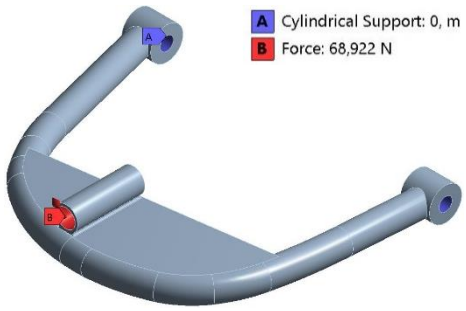


Figure 2. Boundary conditions of the first analysis of the current model.

### 2.2. Topology optimization of the control arm

For the purpose of finding an optimal shape for the suspension control arm, an oversized model was designed and its stress distribution was calculated. This geometry was used to carry out the topology optimization, eliminating material in areas with low stress. Then, the optimized model was analyzed.

Initially, the material and geometry of the control arm were defined. The material selected was nylon and the mechanical properties used are presented in Table 3. As this part is to be built by additive manufacturing with a triangular fill pattern and a 37% fill density, these properties do not correspond to the nylon filament. For the calculation of the properties, tensile values obtained in previous studies were taken as reference (Markforged, n.d.-c) (Beltrán, 2017). In this way, interpolations were made between the values of 20% and 50% for a triangular pattern. From these interpolations, the properties for 37% were obtained.

Table 3. Printed nylon mechanical properties.

| **Property** | **Value** |
|---|---|
| Tensile Ultimate Strength | 18.5 MPa |
| Young's Modulus | 248.5 MPa |
| Poisson's Ratio | 0.47 |
| Bulk Modulus | 1294 MPa |
| Shear Modulus | 84.6 MPa |

The geometry of the oversized part was based on the control arm of the buggy. From this vehicle, the distances between the supports were fixed. A part of similar size but with a flat shape was modeled, tailored for additive manufacturing. For the optimization process, the boundary

conditions of the first analysis of the current model were chosen because they produced higher values of stress. The geometry and boundary conditions used are shown in Figure 3.

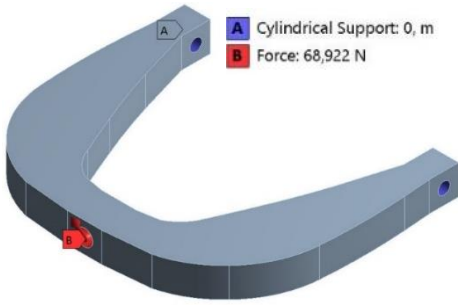


Figure 3. Oversized geometry and boundary conditions.

To perform the topology optimization, it was necessary to establish an optimization region, objectives and constraints. The optimization region was the complete body excluding the areas where the boundary conditions were applied. As objectives, compliance, mass or volume could be selected to minimize. For this analysis, as response constraints, the mass, the volume, global von Mises stress, local von Mises stress, displacement or reaction force could be selected. And, also manufacturing constraints could be added. In this case, the objective was to minimize compliance and the constraint was a mass reduction fixed to 30%.

The topological optimization solver approaches a stationary point where all constraints are satisfied within a tolerance of 0.1 percent of the defined bound. Next, the methodology to get the solution of the optimization is explained (ANSYS Inc., 2018). To simplify the notation, it is assumed that only one constraint *c* exists. The optimality conditions of the topology optimization problem can be stated with the following equation:

$$\|\nabla L(\rho, \mu)\| = 0, \quad (1)$$

where $L(\rho, \mu)$ denotes the Lagrange function defined by:

$$L(\rho, \mu) = f(\rho) - \mu c(\rho), \tag{2}$$

where μ is the Lagrange multiplier corresponding to the constraint $c$, and $f$ is the objective function to be either maximized or minimized. The solver will stop as soon as the desired tolerance is achieved, where: $\in > 0$, as defined here:

$$\|\nabla L(\rho, \mu)\| = \in \tag{3}$$

Because approaching this stationary point can require a large number of iterations, a relaxed convergence criterion is used. The optimization stops as soon as the following equation has three successive iterations. In this equation, $\rho_i$ denotes the vector of pseudo densities of the $i - th$ iteration.

$$\left| \frac{f(\rho_i) - f(\rho_{i-1})}{f(\rho_i)} \right| \leq \in \tag{4}$$

Note that three successive iterations are considered as the underlying solver is stabilized by a line search procedure. This line search procedure might lead to small changes with respect to the pseudo densities as well as small changes to the objective function. It is possible that the convergence tolerance is satisfied for one iteration but the next iteration leads to a significant improvement of the objective function. Due to the relaxed stopping criterion, the optimization might terminate too early. In this case, the optimization should be rerun with a smaller tolerance.

After carrying out the optimization, a faceted body is generated. This means it only describes the surface geometry but does not consider common attributes like color, texture or other. For the analysis of the optimized model, the same material properties and boundary conditions of the oversized model were used. But, the geometry was based on the result of the optimization process. A reconstruction process of the faceted geometry was carried out to generate a simpler solid body

and, thus, facilitate the obtaining of the stress and displacement distributions of the optimized shape. This reconstruction was carried out from the curves of the cross sections of the faceted body that resulted from the optimization, as illustrated in Figure 4. From these curves, surfaces were created to later generate a solid body.

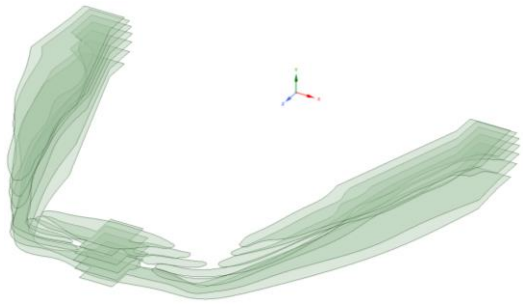

Figure 4. Surfaces of the cross sections of the faceted body.

### 2.3. Manufacturing and validation

The control arm was constructed with continuous fiber reinforcement using the Mark Two Markforged printer. For the printing process, the 3D model illustrated in Figure 5 was utilized. Fiber reinforced parts have greater strength, stiffness, and durability. They also maintain the heat resistance, chemical resistance, and print quality of their thermoplastic matrix material. Markforged uses a combination of Fused Filament Fabrication (FFF, also known as FDM) printing and Continuous Fiber Fabrication (CFF) to lay down long strand fibers in conventionally printed thermoplastic parts. This technology is also extrusion based and prints via a secondary nozzle, but instead of melting the whole filament, it uses the heat of its nozzle to ‘iron’ down fibers into a thermoplastic layer. Fibers do not melt, instead, they are captured by the thermoplastic matrix in a

similar way that thermoset adhesives like epoxy capture fibers in traditional fiber fabrication methods (Markforged, n.d.-a).

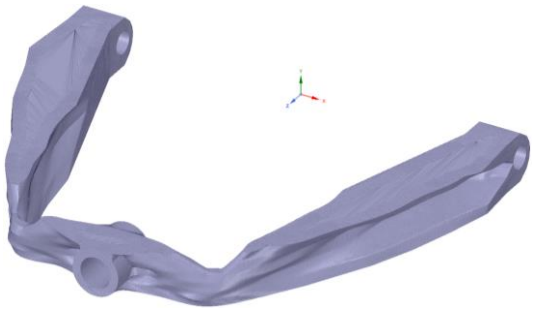

Figure 5. 3D model for printing.

The materials available for the matrix were nylon and onyx, which is nylon thermoplastic infused with chopped carbon fiber, and for the reinforcement, fiberglass, Kevlar and carbon fiber. Table 4 shows some of the properties of the fiber materials that can be used for 3D printed parts. The material selected for the matrix was nylon and fiberglass for the reinforcement. Fiberglass increases the strength of the part and gives it enough stiffness. Besides, it is the most effective material considering its cost.

Table 4. Fiber materials properties.

| **Property** | **Carbon fiber** | **Fiberglass** | **Kevlar** |
|---|---|---|---|
| Tensile Ultimate Strength (MPa) | 700 | 590 | 610 |
| Young's Modulus (GPa) | 54 | 21 | 27 |
| Flexural Strength (MPa) | 470 | 210 | 190 |
| Flexural Modulus (GPa) | 51 | 22 | 26 |
| Density ($g/cm^3$) | 1.4 | 1.6 | 1.25 |

Source. Markforged (Markforged, n.d.-c).

Four fiberglass layers were added into the control arm to enhance its stiffness and strength. The printing parameters used are presented in Table 5. The orientation of the fiber is illustrated in Figure 6. Two of these layers of fiber were located on the top of the control arm and the other two on the bottom, next to the roof and floor layers. These areas were chosen because they were the most loaded, where a greater amount of material was required, according to the topology optimization. Also, the recommendations of the printer manufacturer for the design of 3D printed composites were taken into account (Markforged, n.d.-b). These recommendations include the location of the fiber layers, the number of fiber layers and the use of pins or metal inserts, which will be explained later.

Table 5. Printing parameters used.

| **Parameters** | **Setting** |
|---|---|
| Fill pattern | Triangular |
| Fill density | 37% |
| Roof and floor layers | 4 |
| Wall layers | 2 |
| Total fiber layers | 4 |
| Fiber fill type | Isotropic fiber |
| Concentric fiber rings | 3 |

(a) (b)

Figure 6. Fiber orientation.

The build volume of the Mark Two printer is 320 mm x 132 mm x 154 mm. But, this was not large enough for the complete control arm. Thus, the part was divided into two parts and they were joined with the Loctite® 401 instant adhesive, as recommended by Markforged. This product is designed for the assembly of difficult-to-bond materials which require uniform stress distribution and strong tension and/or shear strength. The product provides rapid bonding of a wide range of materials, including metals, plastics, and elastomers. It is also suited for bonding porous materials (Henkel Corporation, 2012).

Additionally, it was required to reduce wear due to friction with the other vehicle parts. For this reason, three brass inserts were added. Figure 7 shows the brass inserts that were fabricated for this purpose. These inserts were built with diameters greater than those of the holes and were introduced with heat after the printing was made. Therefore, it was necessary to heat the inserts so

that they could melt part of the control arm as they entered. The places where the three inserts were settled were the connections with the chassis and the ball joint.

Figure 7. Brass inserts.

After printing the two parts of the control arm, joining them and introducing the inserts, the validation of the design was carried out. For this, the printed control arm was tested in the buggy car by assembling it on the suspension system.

## 3. Results

### 3.1. Current control arm model

The results of the reaction forces in the lower control arm are shown in Figure 8. As expected, the forces in the *z*-component were the most significant, and the *x*-components were almost nil. Although, all of them were low.

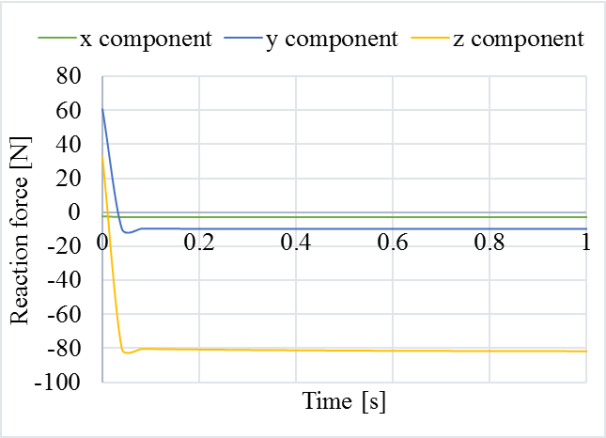


Figure 8. *x*, *y* and *z*-component of the force due to the contact with the ball joint.

The equivalent von Mises stress distribution resulted from the first analysis had a maximum value of approximately 22 MPa and the second had a maximum of 20 MPa. Both values are low taking into account the structural steel strength. Figure 9a and Figure 9b show the results of the first and second analyzes, respectively.

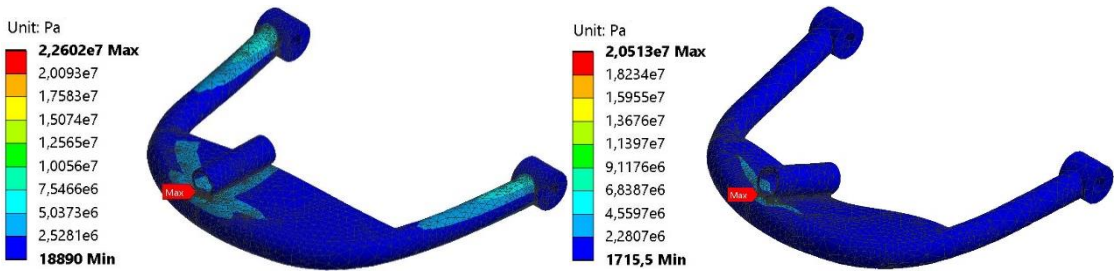


(a) (b)

Figure 9. First (a) and second analysis (b) stress distribution.

Additionally, the total displacement for the first analysis is shown in Figure 10a, and for the second in Figure 10b. The maximum value for the first analysis was approximately 5e-5 m and for the second 1e-5 m. It is observed that the maximum values of the total displacement, in both cases,

occurred at distinct regions of the control arm, which is explained by the different direction of the force applied in each case.

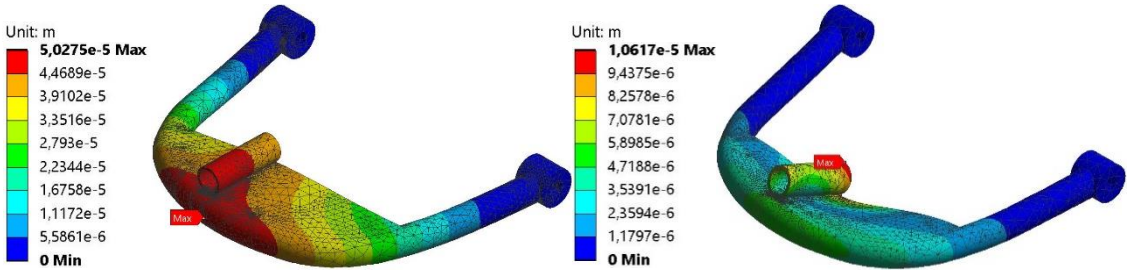


(a) (b)

Figure 10. First (a) and second analysis (b) total displacement.

### 3.2. Topology optimization of the control arm

As previously mentioned, in order to carry out the process of shape optimization, an oversized control arm was designed to later remove the zones that presented low stresses. Figure 11 shows the equivalent von Mises stress of this oversized part, the maximum value was near 3 MPa.

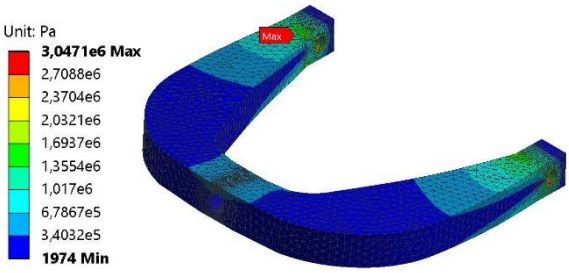


Figure 11. Stress distribution of the oversized model.

To achieve the optimal shape it was necessary to perform 29 iterations. The constraint which was to retain the 30% of mass was reached quickly but more iterations were required for the convergence. The result obtained from the optimization process is shown in Figure 12.


Figure 12. Optimization result.

The geometry resulting from the topology optimization, Figure 12, was post-processed to obtain a non-faceted reconstructed geometry, which facilitates the design and manufacture of the final prototype. Figure 13a presents the faceted body generated with the optimization process (gray) compared with the reconstructed solid body (green). Furthermore, Figure 13b shows the deviation between these bodies, where, both the exterior and interior differences between the two geometries can be seen. The tolerance used was 0.01 mm. The maximum interior deviation was 5.01 mm and the maximum exterior deviation was 3.78 mm. It can be seen that they are very similar, and the complexity of this reconstructed solid body is much less than if the facets had been automatically converted to a solid body.

When analyzing the optimized reconstructed geometry, both the stress and the total displacement distributions were calculated. The equivalent von Mises stress distribution is shown in Figure 14a and total displacement in Figure 14b. The maximum stress was 2.7 MPa and the maximum displacement was 9.3 mm. Therefore, with respect to the current control arm model, the

difference between the maximum stress values is not significant, but greater differences are observed in terms of total displacement.

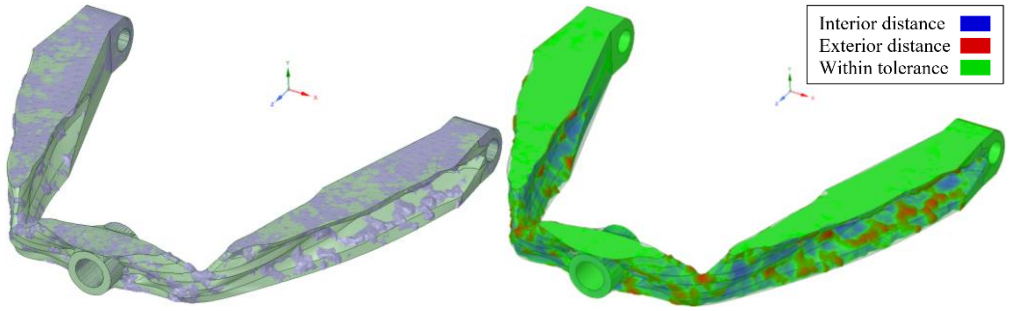


(a) (b)

Figure 13. Optimization result vs reconstructed part (a) and its deviation (b).

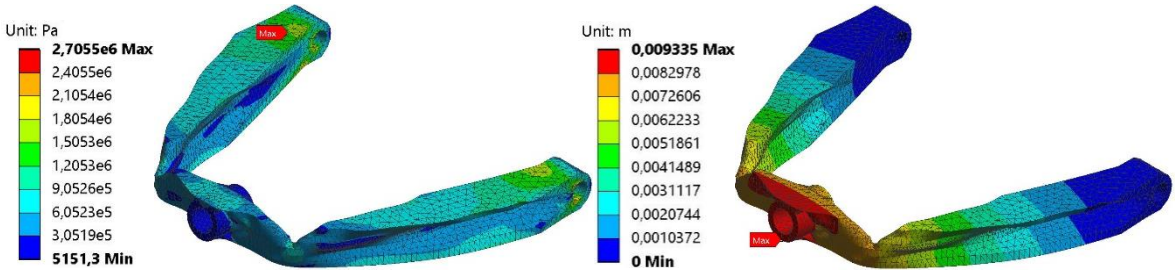


(a) (b)

Figure 14. Stress (a) and total displacement (b) distributions of the optimized model.

### 3.3. Manufacturing and validation

The optimized geometry was manufactured in nylon by additive manufacturing with fiberglass reinforcement using the parameters in Table 5. The parts in which the control arm was divided are shown in Figure 15. The printings were satisfactory although the dimensions were not accurate, especially those of the holes. It was also observed that in the areas where support material had to

be removed, the quality of the surface was rough. Table 6 presents the details of each of these parts.

Figure 15. Parts of the printed control arm.

Table 6. Printed parts details.

| **Part detail** | **Part 1** | **Part 2** |
|---|---|---|
| Print time | 19h 59m | 19h 35m |
| Material cost | 24.49 USD | 23.77 USD |
| Mass of part | 84.41 g | 82.12 g |
| Plastic volume | 100.07 $cm^3$ | 97.44 $cm^3$ |
| Fiber volume | 2.23 $cm^3$ | 2.12 $cm^3$ |

The final printed control arm (after joining the two parts and introduce the brass inserts) is presented in Figure 16a. The weight of this final part was 216 g, which is significantly lower compared to the 835 g of the steel control arm. The assembled suspension of the buggy car with the printed part can be seen in Figure 16b. The control arm was mounted easily in the suspension, its dimensions were adequate for normal operation and to keep the wheel in vertical position. The duration of the test was approximately twenty minutes and no failure was observed in the part. Figure 16c shows the control arm after the test.

(a) (b) (c)

Figure 16. Printed control arm before (a), during (b) and after (c) the test.

## 4. Conclusions

In the present work, the topology optimization of a lower control arm of a buggy car produced by additive manufacturing was performed. First, a finite element analysis of the lower control arm of the suspension system was done to obtain the stress and displacement fields. For this purpose, the forces on the lower arm were calculated using a kinematic model. The resulting loading conditions of the control arm were low, the maximum force was near of 83 N and, therefore, there were also low stresses, close to 20 MPa. These results showed that it was feasible to optimize the shape of the arm to save material and lighten the part. Additionally, regarding the material, a change from steel to a reinforced composite printed by additive manufacturing was proposed.

The optimization process was carried out for the control arm using topology optimization. The stress values were decreased from 20 MPa to almost 3 MPa, and a reduction of almost 75% of the weight of the control arm was achieved, compared with the initial steel configuration. In terms of automotive parts, this means lower consumption of energy by the vehicle, thus, requiring less fuel.

Therefore, this manufacturing process together with the topology optimization approach can yield significant weight reductions and also high values of strength when incorporating fiber.

On the other hand, it would be appropriate to deepen more in the study of the loads to which the part is subjected, since in this study only the weight of the vehicle and passengers was taken into account, but there are other conditions that may also affect the part.

## References

Al Abadi, H., Thai, H. T., Paton-Cole, V., & Patel, V. I. (2018). Elastic properties of 3D printed fibre-reinforced structures. *Composite Structures*, *193*(February), 8–18. https://doi.org/10.1016/j.compstruct.2018.03.051

Allaire, G., Dapogny, C., Faure, A., & Michailidis, G. (2017). Shape optimization of a layer by layer mechanical constraint for additive manufacturing Optimisation. *C. R. Acad. Sci. Paris, Ser. I*, *355*(6), 699–717. https://doi.org/10.1016/j.crma.2017.04.008

ANSYS Inc. (2018). ANSYS® Academic Research Mechanical Release 18.1.

Beltrán, S. (2017). *Caracterización y predicción de las propiedades a tensión de componentes impresos en 3D con refuerzo de fibras*. Universidad Industrial de Santander.

Blok, L. G., Longana, M. L., Yu, H., & Woods, B. K. S. (2018). An investigation into 3D printing of fibre reinforced thermoplastic composites. *Additive Manufacturing*. https://doi.org/10.1016/j.addma.2018.04.039

Bouazara, M. (2009). Improvement in the Design of Automobile Upper Suspension Control Arms Using Aluminum Alloys. *Damage and Fracture Mechanics*, 101–112. https://doi.org/10.1007/978-90-481-2669-9_11

Caminero, M. A., Chacón, J. M., García Moreno, I., & Reverte, J. M. (2018). Interlaminar bonding performance of 3D printed continuous fibre reinforced thermoplastic composites using fused deposition modelling. *Polymer Testing*, *68*(July), 415–423. https://doi.org/10.1016/j.polymertesting.2018.04.038

Chen, J., Ahmad, R., Suenaga, H., Li, W., Sasaki, K., Swain, M., & Li, Q. (2015). Shape

optimization for additive manufacturing of removable partial dentures - A new paradigm for prosthetic CAD/CAM. *PLoS ONE*, *10*(7), 1–17. https://doi.org/10.1371/journal.pone.0132552

Dama, K., Malyala, S., Babu, V., Rao, R., & Shaik, I. (2017). Development of Automotive FlexBody Chassis Structure in Conceptual Design Phase using Additive Manufacturing. *Materials Today: Proceedings*, *4*(9), 9919–9923. https://doi.org/10.1016/j.matpr.2017.06.294

Dassault Systemes. (2017). Solidworks 2017.

Gao, W., Zhang, Y., Ramanujan, D., Ramani, K., Chen, Y., Williams, C. B., … Zavattieri, P. D. (2015). The status, challenges, and future of additive manufacturing in engineering. *Computer-Aided Design*, *69*, 65–89. https://doi.org/10.1016/j.cad.2015.04.001

Hegab, H. A. (2016). Design for additive manufacturing of composite materials and potential alloys: a review. *Manufacturing Review*, *3*, 11. https://doi.org/10.1051/mfreview/2016010

Henkel Corporation. (2012). Loctite® 401™ Technical Data Sheet.

Hofstätter, T., Pedersen, D. B., Tosello, G., & Hansen, H. N. (2017). Applications of Fiber-Reinforced Polymers in Additive Manufacturing. *Procedia CIRP*, *66*, 312–316. https://doi.org/10.1016/j.procir.2017.03.171

Karunakaran, K., Bernard, A., Suryakumar, S., Dembinski, L., & Taillandier, G. (2012). Rapid manufacturing of metallic objects. *Rapid Prototyping Journal*, *18*(4), 264–280. https://doi.org/10.1108/13552541211231644

Khode, A. P., Senthilkumar, K., Patil, B. S., Kulkarni, N., & Trikande, M. W. (2017). Shape Optimization and Weight Reduction of Seat Structure for Wheeled Armoured Amphibious Combat Vehicle. In *Materials Today: Proceedings* (Vol. 4, pp. 1917–1926). Elsevier Ltd.

https://doi.org/10.1016/j.matpr.2017.02.037

Leary, M., Merli, L., Torti, F., Mazur, M., & Brandt, M. (2014). Optimal topology for additive manufacture: A method for enabling additive manufacture of support-free optimal structures. *Materials and Design*, *63*, 678–690. https://doi.org/10.1016/j.matdes.2014.06.015

Lederman, D., Messina, J., Pienknagura, S., & Rigolini, J. (2014). *Latin American Entrepreneurs: Many Firms but Little Innovation*. Washington, DC: World Bank. https://doi.org/10.1596/978-1-4648-0012-2

Mark, G. T., & Gozdz, A. S. (2015). Three dimensional printer with composite filament fabrication. United States. https://doi.org/10.1016/j.(73)

Markforged. (n.d.-a). 3D Printing Materials. Retrieved January 8, 2019, from https://markforged.com/learn/articles/3d-printing-materials/

Markforged. (n.d.-b). 3D printing with composites design guide. Retrieved December 21, 2018, from https://s3.amazonaws.com/mf.product.doc.images/Composites_DesignGuide/CompositesDesignGuide_V1-1.pdf

Markforged. (n.d.-c). Materials. Retrieved October 16, 2018, from https://support.markforged.com/hc/en-us/articles/209934406

Melenka, G. W., Cheung, B. K. O., Schofield, J., Dawson, M. R., & Carey, J. P. (2016). Evaluation and prediction of the tensile properties of continuous fiber-reinforced 3D printed structures. *Composite Structures*, *153*, 866–875. https://doi.org/10.7939/R3PC2TP4F

Ngo, T., Kashani, A., Imbalzano, G., Nguyen, K., & Hui, D. (2018). Additive manufacturing (3D printing): A review of materials, methods, applications and challenges. *Composites Part B*, *143*, 172–196. https://doi.org/10.1016/j.compositesb.2018.02.012

Ning, F., Cong, W., Qiu, J., Wei, J., & Wang, S. (2015). Additive manufacturing of carbon fiber reinforced thermoplastic composites using fused deposition modeling. *Composites Part B: Engineering*, *80*, 369–378. https://doi.org/10.1016/j.compositesb.2015.06.013

Parandoush, P., & Lin, D. (2017). A review on additive manufacturing of polymer-fiber composites. *Composite Structures*, *182*, 36–53. https://doi.org/10.1016/j.compstruct.2017.08.088

Paris, H., Mokhtarian, H., Coatanéa, E., Museau, M., & Ituarte, I. F. (2016). Comparative environmental impacts of additive and subtractive manufacturing technologies. *CIRP Annals - Manufacturing Technology*, *65*(1), 29–32. https://doi.org/10.1016/j.cirp.2016.04.036

Sauer, M. J. (2018). *Evaluation of the Mechanical Properties of 3D Printed Carbon Fiber Composites*. South Dakota State University.

Song, B. C., Park, Y. C., Kang, S. W., & Lee, K. H. (2009). Structural optimization of an upper control arm, considering the strength. *Proceedings of the Institution of Mechanical Engineers, Part D: Journal of Automobile Engineering*, *223*(6), 727–735. https://doi.org/10.1243/09544070JAUTO1090

Song, X. G., Jung, J. H., Son, H. J., Park, J. H., Lee, K. H., & Park, Y. C. (2010). Metamodel-based optimization of a control arm considering strength and durability performance. *Computers and Mathematics with Applications*, *60*(4), 976–980. https://doi.org/10.1016/j.camwa.2010.03.019

Spowart, J. E., Gupta, N., & Lehmhus, D. (2018). Additive Manufacturing of Composites and Complex Materials. *Jom*, *70*(3), 272–274. https://doi.org/10.1007/s11837-018-2742-2

Vayre, B., Vignat, F., & Villeneuve, F. (2012). Designing for additive manufacturing. *Procedia CIRP*, *3*(1), 632–637. https://doi.org/10.1016/j.procir.2012.07.108

Vinodh, S., & Jayakrishna, K. (2011). Environmental impact minimisation in an automotive component using alternative materials and manufacturing processes. *Materials and Design*, *32*(10), 5082–5090. https://doi.org/10.1016/j.matdes.2011.06.025

Walton, D., & Moztarzadeh, H. (2017). Design and Development of an Additive Manufactured Component by Topology Optimisation. In *CIRP Design* (Vol. 60, pp. 205–210). Elsevier B.V. https://doi.org/10.1016/j.procir.2017.03.027